The effects of screen sizes on the surface properties of tepered steel treated by active screen plasma nitriding

Kovács D., Kemény A., Bonyár A., Dobránszky J.

Accepted for publication in IOP Conference Series: Materials Science and Engineering
Published in 2018
DOI: 10.1088/1757-899X/416/1/012040

The Effects of Screen Sizes on the Surface Properties of Tepered Steel Treated by Active Screen Plasma Nitriding

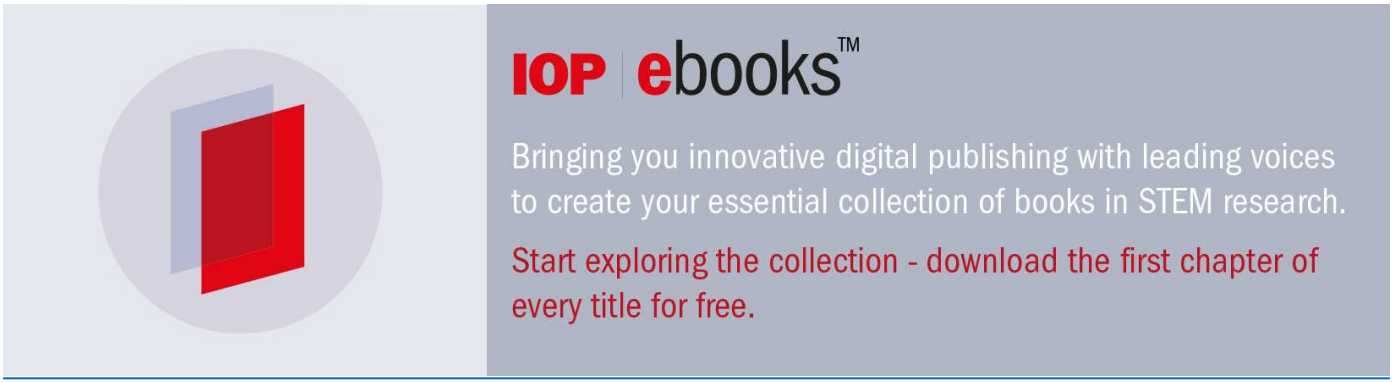

IOP Conf. Series: Materials Science and Engineering **416** (2018) 012040 doi:10.1088/1757-899X/416/1/012040

The Effects of Screen Sizes on the Surface Properties of Tepered Steel Treated by Active Screen Plasma Nitriding

D Kovács[1], A Kemény[1], A Bonyár[2] and J Dobránszky[3]

[1] Budapest University of Technology and Economics, Faculty of Mechanical Engineering, Department of Material Science and Engineering,
1111, Budapest, Műegyetem rakpart 3, Hungary.
[2]Budapest University of Technology and Economics, Department of Electronics Technology,
1111, Budapest, Egry József street 18, Hungary
[3] MTA–BME Research Group for Composite Science and Technology,
1111, Budapest, Műegyetem rakpart 3, Hungary

[*]Corresponding author dorina@eik.bme.hu

Abstract. Active screen plasma nitriding (ASPN) is a novel thermochemical surface treatment which has many specialities compared to the conventional direct current plasma nitriding (DCPN). The edge effect is eliminated, the hardness and layer thickness on the surface are homogeneously distributed. In this study, 42CrMo4 alloyed steel was treated with different screen sizes (screen diameter, hole size) active screen plasma nitriding. The parameters of treatment are similar in all cases (4 hours at 490°C and 2,2 torr). The nitrided samples were characterized by atomic force microscope (AFM) to analyse the roughness of the surface. The cross-section hardness of the samples and the thickness of the nitrided layers were also measured.

1. Introduction

The nitriding process is widely used for improving the hardness and the wear resistance of steels. DCPN has become a standard industrial technology, but it has some technological issues such as edge effect and hollow cathode effect [1–3]. Over the years, ASPN appeared in the plasma nitriding treatment processes. The main advantages are based on the replacement of the glow discharge region. This means, that the plasma forms on the screen, instead of the workpiece, which causes homogeneous hardness and layer thickness on the surface of the specimen, therefore the issues of the DCPN are eliminated. Considering that the plasma is formed only on the screen, and the worktable is isolated from the voltage source, the samples are heated by radiation. ASPN also generates nitrogen mass transfer to the surfaces of the specimens [4, 5]. Several researchers have reported the effects of the nitriding parameters, such as the distance between the screen and the sample [6–8], the effect of different screen sizes [9–11] on the surface roughness [12–16] and also wear and corrosion resistance improvement [17–20].

Surface roughness parameters, which can be quantified with AFM, are frequently used as a typical measurement of mechanical surface properties. In our particular case, the interaction between ions and the sample surface during the sputtering corresponds to the variation of the roughness [21–23]. The wear and corrosion resistance are depending on the base material, but these material properties are not evaluated in this research.

The aim of this research is to investigate the influence of the active screen hole sizes on the layer thickness, cross-section hardness profile and most importantly the surface roughness of the active screen plasma nitrided samples.

2. Materials and methods

In this study, tempered 42CrMo4 low alloy steel was used with the following chemical compositions shown in Table 1. The sample disks were 20 mm in diameter and 6 mm in thickness. The surface of the samples was mechanically ground with 80 to 2500-grit SiC paper and polished with 3 μm diamond suspension. The samples were cleaned with acetone and dried before placed in the vacuum chamber.

Table 1. Chemical composition of materials in wt.%

	C	Si	Mn	P	S	Cr	Mo
42CrMo4	0.38 – 0.45	≤0.4	0.6 – 0.9	≤0.025	≤0.035	0.9 – 1.2	1.5 – 0.3

The active screen was made of 1.0330 type steel. The screen dimensions were ∅100×85 mm with ∅5 mm, ∅18 mm and ∅45 mm holes and the wall thickness was 0.8 mm. Figure 1 shows the schematic workspace of the chamber and the screens with the different hole diameters and the distance of their centers. All treatments were carried out using the same parameters as shown in Table 2 and following the same procedures. First, the chamber was pumped to a base pressure of 2×10^{-1} torr, then the chamber was flushed with argon. After the flushing, the pressure was set to 2,2 torr with the nitriding gas. The plasma was produced on a negatively polarized screen (cathode) and the anode (base of the chamber), which was held at ground potential. The temperature was monitored using an isolated K-type thermo-couple under the workpiece. After the nitriding process, the workpiece was cooled down from the treat-ment temperature to the room temperature.

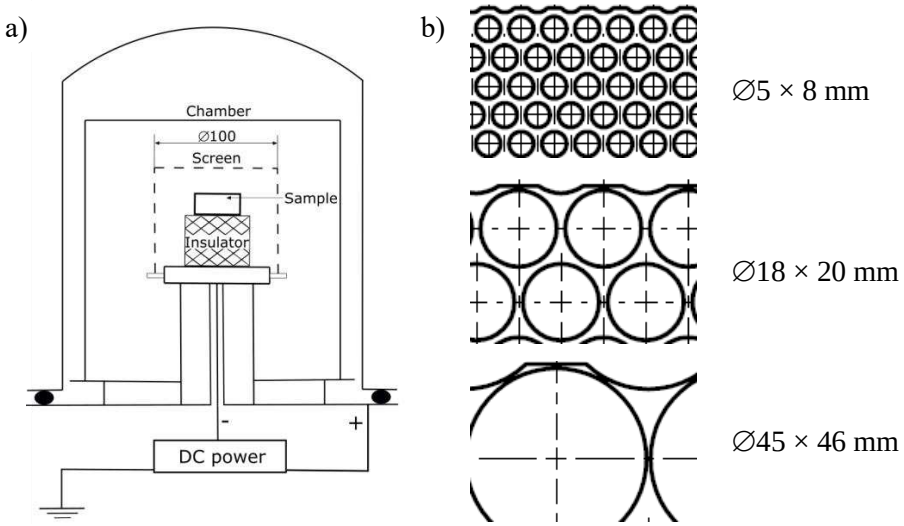

Figure 1.a) Schematic diagram of the ASPN chamber
b) Hole diameters of active screens

Table 2. Parameters of plasma nitriding

Voltage (V)	Current (A)	Gas mixture N_2:H_2(%)	Temperature (°C)	Pressure (torr)	Time (h)
490 – 540	0.9 – 1.5	25:75	490	2.2	4

Scanning electron microscope (SEM) was used to examine the morphology of the samples and measure the thickness of the nitrided layer. For the microhardness measurement Buehler IndentaMet 1105 equipment was used with Vickers head. The measuring load was 10 g for 11 s time. Contact mode AFM images were taken with a Veeco (lately Bruker) diInnova scanning probe microscope (SPM) with Bruker DNP-10 probes, using the longest cantilever with the smallest spring constant (k = 0.03 N/m). The sampling rate of the image acquisition was 512x512 with 1 Hz scan rate. The obtained images were post-processed with the Gwyddion 2.36 software [24]. Only standard background correction was applied on the images to remove piezo movement and sample tilt effects.

3. Results and discussion

The results of the different hole sized ASPN processes are compared with DCPN on the same nitriding parameters.

3.1. Thickness and hardness measurements

Scanning electron microscope was used to determine the depth of the compound zone. Figure 2 shows the cross-sections of the samples. The layer thickness was 5.8 µm with DCPN, 3.2 µm with ∅5 mm holes of AS (active screen), 5.5 µm with ∅18 mm holes of AS and 5. µm with ∅45 mm holes of AS. The layer thickness doesn't increase significantly when the hole size is increased over ∅18 mm. It means that there is a critical transition hole size between ∅5 mm and ∅18 mm which needs further investigation. The highest thickness is at DCPN treatment because of the direct heating with current. However, in this case the layer is not uneven, and nitride networks were founded at some place of the diffusion zone along the grain boundaries.

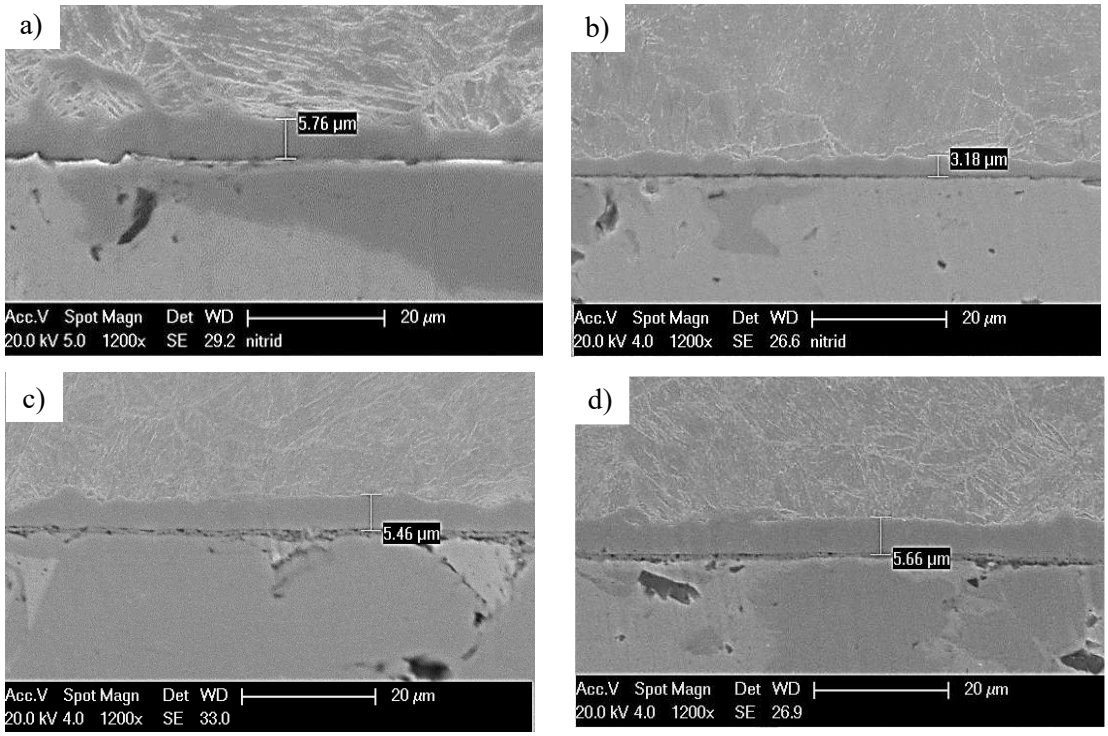

Figure 2. Compound layer thickness of steel 42CrMo4 a) DCPN, b) ∅5 mm holes of AS, c) ∅18 mm holes of AS, d) ∅45 mm holes of AS treated samples

Figure 3 shows the cross-section hardness profiles of the investigated samples and the maximum hardnesses are found in Table 3. Each curve is made from 3 different measurements on different places

of the cross-section, but all started from the layer, through the diffusion zone, towards the base material. The standard deviation is also shown on the diagram in every point.

Table 3. Maximum hardnesses of nitrided samples

	DCPN	∅5 mm holes of ASPN	∅18 mm holes of ASPN	∅45 mm holes of ASPN
HV0.01	1050	787	912	698

From the diagram it can be read that according to the layer thickness values, the DCPN sample has the highest hardness. This seems good, but the DCPN method always creates an edge effect, where the layer is not uniform with the other parts of the sample and the hardness values near the edge effect are differ from the common hardness of the nitrided sample [6, 8, 20]. It is also interesting, that the ∅18 mm hole size screen effects the highest hardness values among the ASPN treated samples. It can be declared as an optimum among the other screens. This statement is also backed by the layer thickness measurements. The layer thickness depends on the quantity of formed nitrides. Nitrides have significantly higher hardness than the raw material, so theoretically the thicker layers should have higher hardness. However, the hardness values of the ∅45 mm hole size ASPN treated sample should be considered. A possible explanation for the lower values, is that the holes are too large in the screen, so it is not able to create a fully even layer where there is and open area of the screen. Although this possibility should be examined further.

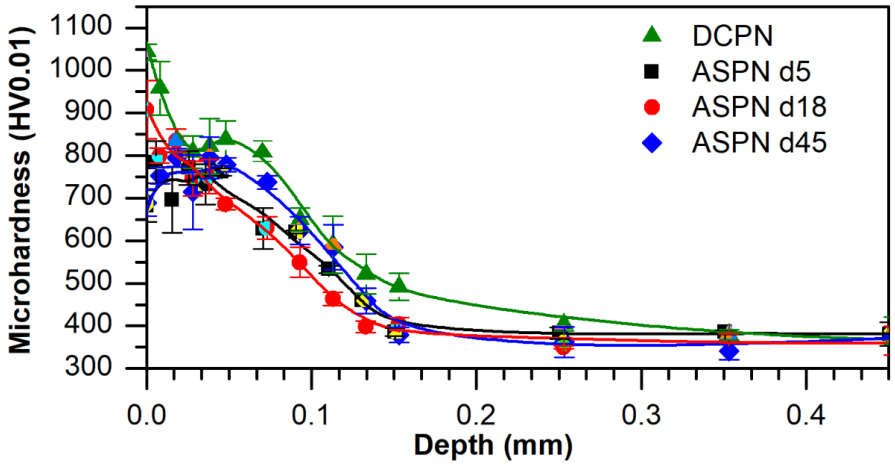

Figure 3. Hardness profile of plasma nitrided samples

3.2. Surface roughness measurements with AFM

The surface topography of the samples was investigated by AFM, as shown in figure 4. It can be clearly seen that the surface roughness of the nitrided samples can even be 30-40 times higher than the polished reference sample (S_a is 0.75±0.05 nm for the reference, 15±0.05 nm for the DCPN sample and is between 35-40 nm for the ASPN samples, measured on 2×2 μm images). The ∅18 mm hole size screen has the highest roughness. If the dimension of the hole size is increasing, the roughness is also increasing until the critical transition size. Each results of previous measurements confirm the ∅18 mm hole size screen is a transition size among the hole size dimensions. It has to be noted that the surface roughness is not sufficient alone to conveniently characterize the effect of nitriding. As can be seen in figure 4, the surface after the treatment is structured in different levels. Besides the grains caused by the process, we can observe surface waviness with hills and valleys (especially for the DCPN treated samples in figure 4 c)-d)), and also larger, complex structures (which resemble aggregated grains, most visible in the 10×10 μm images of figure 4 e)-j) for the ASPN samples with larger hole diameters). This means, that the treated surfaces have different characteristic features depending on the technological parameters,

and since these features have different spatial frequency, based on the selected scan-size, the measured surface roughness values will be affected differently. By using smaller scan sizes it is possible to focus on the grainy nitride structures. It is clear that the ASPN samples have significantly larger grain sizes compared to the DCPN sample, moreover, the treatment with ∅18 mm hole size resulted in the largest average grains. At larger scan sizes the mentioned complex structures define the surface roughness, which increases with a factor of 1.4-2.3 by increasing the scan size to 10×10 μm from 2×2 μm, depending on the samples. These structures with smaller spatial frequency could also be attributed to aspects of the treatment, but their detailed characterization is out of the scope of the current paper.

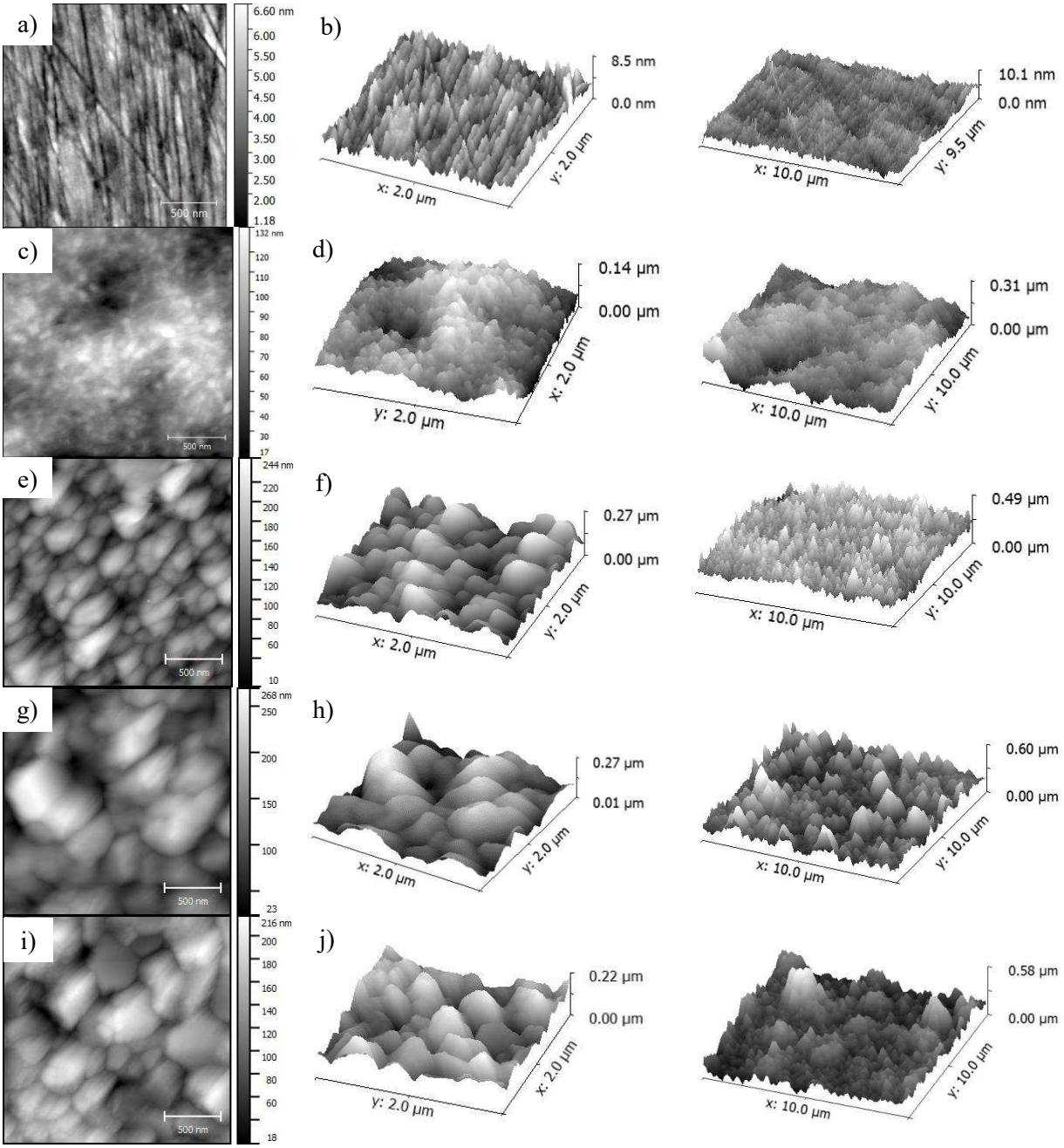

Figure 4. Contact-mode 2D and 3D AFM topography images made on a)-b) polished, c)-d) DCPN treated, e)-f) ∅5 mm holes of AS treated, g)-h) ∅18 mm holes of AS treated, i)-j) ∅45 mm holes of AS treated samples.

4. Conclusions

- The highest thickness is obtained by using DCPN treatment, but the edge effect causes an uneven layer thickness. It seems that the ASPN process has a critical transition from the point of view of the screens hole sizes, which treatment influences the layer thickness.
- Also, the DCPN treatment resulted the highest hardness in the nitrided layer. The ASPN treated samples have similar hardness, but their maximum hardnesses are lower than the DCPN treated sample. After all, the highest hardness formed when the screen with ∅18 mm holes was used.
- The surface roughness of the nitrided samples can even be 30-40 times higher than the polished originals, depending on the process, but besides the nitride grains the ASPN samples show characteristic features with smaller spatial frequency. The relation of these structures with the technological parameters should be investigated in more detail in the future.
- The AFM investigation of the surfaces showed that the sample treated by using an ∅18 mm hole size screen has the highest average grain size.
- All things considered, ∅18 mm hole could be considered as the optimal size of the screen for the ASPN process, based on the investigated samples in this research.

5. References

[1] Andrea S B and Mária K B 2012 *Nitridálás – korszerű eljárások és vizsgálati módszerek Miskolc* (Miskolc: Miskolci Egyetem)
[2] Asm International 1991 Heat Treating *ASM Int. Mater. Park. OH* **4** 860
[3] Pye D 2003 *Practical NITRIDING and Ferritic Nitrocarburizing* (Ohio: ASM International)
[4] Hamann S, Börner K, Burlacov I, Hübner M, Spies H J and Röpcke J 2013 Spectroscopic studies of conventional and active screen N 2-H2 plasma nitriding processes with admixtures of CH 4 or CO2 *Plasma Sci. Technol.* **22**
[5] Yazdani A, Soltanieh M and Aghajani H 2015 Active screen plasma nitriding of Al using an iron cage: Characterization and evaluation *Vacuum* **122** 127–34
[6] Nishimoto A, Nagatsuka K, Narita R, Nii H and Akamatsu K 2010 Effect of the distance between screen and sample on active screen plasma nitriding properties *Surf. Coatings Technol.* **205** 8–11
[7] de Sousa R R M, de Araújo F O, da Costa J A P, Dumelow T, de Oliveira R S and Alves C 2009 Nitriding in cathodic cage of stainless steel AISI 316: Influence of sample position *Vacuum* **83** 1402–5
[8] de Sousa R R M, de Araújo F O, da Costa J A P, de S. Brandim A, de Brito R A and Alves C 2012 Cathodic Cage Plasma Nitriding: An Innovative Technique *J. Metall.* **2012** 1–6
[9] Nishimoto A, Matsukawa T and Nii H 2014 Effect of Screen Open Area on Active Screen Plasma Nitriding of Austenitic Stainless Steel *ISIJ Int.* **54** 916–9
[10] Nishimoto A, Tokuda A and Akamatsu K 2009 Effect of Through Cage on Active Screen Plasma Nitriding Properties *Mater. Trans.* **50** 1169–73
[11] Ahangarani S, Mahboubi F and Sabour A R 2006 Effects of various nitriding parameters on active screen plasma nitriding behavior of a low-alloy steel *Vacuum* **80** 1032–7
[12] Karimzadeh N, Moghaddam E G, Mirjani M and Raeissi K 2013 The effect of gas mixture of post-oxidation on structure and corrosion behavior of plasma nitrided AISI 316 stainless steel *Appl. Surf. Sci.* **283** 584–9
[13] Ganesh Sundara Raman S and Jayaprakash M 2007 Influence of plasma nitriding on plain fatigue and fretting fatigue behaviour of AISI 304 austenitic stainless steel *Surf. Coatings Technol.* **201** 5906–11
[14] Allenstein A N, Lepienski C M, Buschinelli A J A and Brunatto S F 2013 Plasma nitriding using high H2 content gas mixtures for a cavitation erosion resistant steel *Appl. Surf. Sci.* **277** 15–24
[15] Borgioli F, Fossati A, Matassini G, Galvanetto E and Bacci T 2010 Low temperature glow-discharge nitriding of a low nickel austenitic stainless steel *Surf. Coatings Technol.* **204** 3410–7
[16] Hirsch T, Clarke T G R and da Silva Rocha A 2007 An in-situ study of plasma nitriding *Surf.*

Coatings Technol. **201** 6380–6
[17] Köster K, Kaestner P, Bräuer G, Hoche H, Troßmann T and Oechsner M 2013 Material condition tailored to plasma nitriding process for ensuring corrosion and wear resistance of austenitic stainless steel *Surf. Coatings Technol.* **228** S615–8
[18] Li Y, Wang L, Xu J and Zhang D 2012 Plasma nitriding of AISI 316L austenitic stainless steels at anodic potential *Surf. Coatings Technol.* **206** 2430–7
[19] Li Y, Wang L, Shen L, Zhang D and Wang C 2010 Plasma nitriding of 42CrMo low alloy steels at anodic or cathodic potentials *Surf. Coatings Technol.* **204** 2337–42
[20] Alves C, de Araújo F O, Ribeiro K J B, da Costa J A P, Sousa R R M and de Sousa R S 2006 Use of cathodic cage in plasma nitriding *Surf. Coatings Technol.* **201** 2450–4
[21] Li Y, Wang Z and Wang L 2014 Surface properties of nitrided layer on AISI 316L austenitic stainless steel produced by high temperature plasma nitriding in short time *Appl. Surf. Sci.* **298** 243–50
[22] de Sousa R R M, de Araújo F O, Ribeiro K J B, Mendes M W D, da Costa J A P and Alves C 2007 Cathodic cage nitriding of samples with different dimensions *Mater. Sci. Eng. A* **465** 223–7
[23] Öztürk O, Okur S and Riviere J P 2009 Structural and magnetic characterization of plasma ion nitrided layer on 316L stainless steel alloy *Nucl. Instruments Methods Phys. Res. Sect. B Beam Interact. with Mater. Atoms* **267** 1540–5
[24] Hossein A and Behrangi S 1988 *Plasma nitriding of steels* **17**
[25] Hubbard P, Dowey S J, Partridge J G, Doyle E D and McCulloch D G 2010 Investigation of nitrogen mass transfer within an industrial plasma nitriding system II: Application of a biased screen *Surf. Coatings Technol.* **204** 1151–7
[26] Hubbard P, Partridge J G, Doyle E D, McCulloch D G, Taylor M B and Dowey S J 2010 Investigation of nitrogen mass transfer within an industrial plasma nitriding system I: The role of surface deposits *Surf. Coatings Technol.* **204** 1145–50

Acknowledgments
The research reported in this paper was supported by the Higher Education Excellence Program of the Ministry of Human Capacities in the frame of Nanotechnology research area of Budapest University of Technology and Economics (BME FIKP-NANO). This work is partially supported by Richter Gedeon Plc. This research has been partially supported by the ‘‘ÚNKP” program of the Hungarian Government.